

Upconversion in $\text{Er}^{3+}:\text{YAlO}_3$ produced by metastable state absorption

Richard Scheps

Naval Research Council and Gamma Sciences Center, RDT&E Division (N640), Code 734, Sea Orgs, CA 90132, USA

Received 14 August 1996; accepted 31 December 1996

Abstract

Upconversion emission in $\text{Er}:\text{YAlO}_3$ ($\text{Er}:\text{YALO}$) was produced by excitation at wavelengths amongst WOT transitions from the $^4I_{13/2}$ metastable state. Both steady state and time dependent fluorescence measurements are reported, and the energy flow pathway is described. The upconverted pump mechanism is a combination of cross relaxation energy transfer and cross-relaxant assisted two-photon absorption. Upconversion emission from the $^2F_{5/2}$ state in $\text{Er}:\text{YALO}$ was also observed.

1. Introduction

Over 160 nm of 350 nm emission was recently reported [1,2] for an $\text{Er}^{3+}:\text{YAlO}_3$ ($\text{Er}:\text{YALO}$) upconversion laser. The optical conversion efficiency was 17% and is among the highest demonstrated for this type of laser. These results are particularly remarkable in light of the higher photon energy in YAlO_3 compared to fluoride-based hosts such as YLF. Higher photon energies are characteristic of oxide hosts and serve to abrogate the metastable state lifetimes. This lowers the upconversion pump efficiency. For example, only low power, self-pulsed upconversion laser emission has been reported for $\text{Er}:\text{YAG}$ [3] and $\text{Tm}:\text{YAG}$ [4].

Emission in 350 nm results from excitation at wavelengths between 785 and 790 nm. $\text{Er}:\text{YALO}$ is unusual in that upconversion lasing may be produced by three different energy transfer mechanisms. Which of these dominates is determined by the excitation conditions and the specific pump wave-

length used. Two of the upconversion pump mechanisms have been previously identified [1,5] as cooperative energy transfer upconversion and sequential two-photon absorption upconversion. Cooperative energy transfer dominates when the pump wavelength is resonant with transitions from the $^4I_{13/2}$ ground state to the $^4I_{9/2}$ state. Following excitation the ion relaxes to the $^4I_{11/2}$ intermediate state. Cooperative energy transfer between two ions in the $^4I_{11/2}$ state produces an ion in the $^4F_{7/2}$ upper laser state. Sequential two-photon absorption can dominate if in addition to pumping the $^4I_{13/2} \rightarrow ^4I_{9/2}$ transition, simultaneous excitation is provided at a second wavelength to promote ions from the intermediate state to the upper laser level.

A third pump process was reported [2] to produce 350 nm laser emission. This mechanism is distinguished from the other two in that the pump wavelength is resonant with transitions from the $^4I_{13/2}$ metastable state. This pump excitation had been previously assigned [2] to photon-assisted upcon-

tion conditions are identical to those used to produce laser emission [1,2], and this could be verified by inserting an output coupler mirror as illustrated in Fig. 1. A chopper was placed in the pump beam path for the first dependent measurements. Chopping frequencies between 20 and 50 Hz were used.

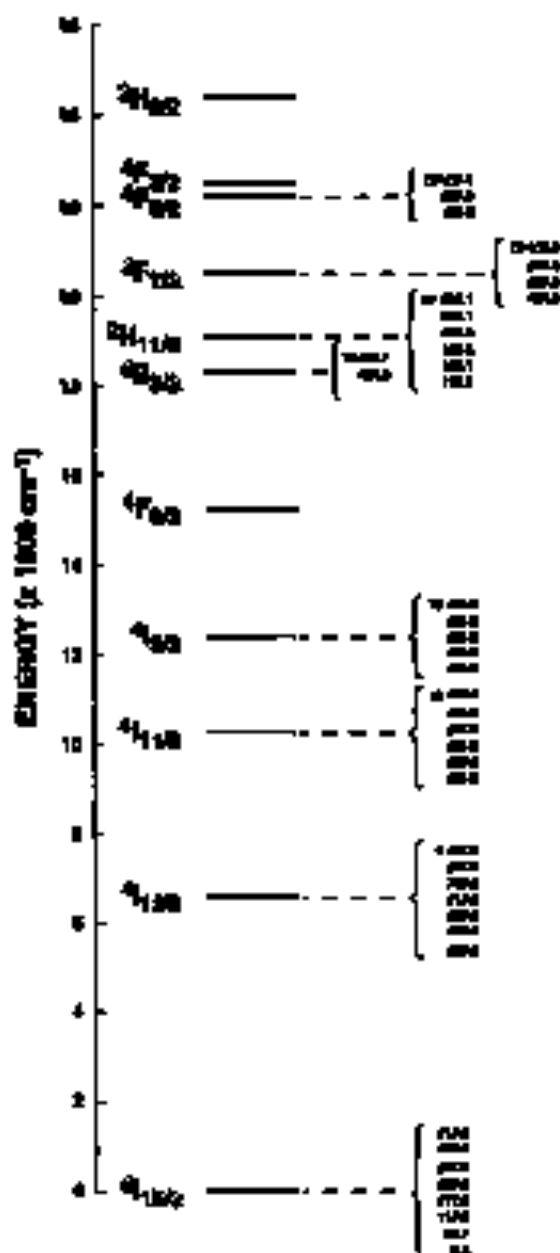
3. Background

A brief summary of the fundamental concepts related to upconversion in Er:YALO is useful to provide a framework for the discussion presented below. A more detailed description of upconversion processes in various materials is available in the literature [6]. A partial energy level diagram is shown in Fig. 2. The term ‘upconversion’ generally refers to processes that produce population in an excited state whose energy exceeds that of the absorbed pump photon. In Er:YALO absorption of light at approximately 600 nm leads to 550 nm emission due to the $^4S_{3/2} \rightarrow ^4I_{11/2}$ transition. Under appropriate conditions upconversion pumping can produce a population inversion, leading to ER-pumped visible laser emission.

Several upconversion pump mechanisms are known to produce laser emission. These include sequential two-photon absorption upconversion, cooperative energy transfer upconversion and photon avalanche upconversion. Sequential two-photon absorption upconversion and cooperative energy transfer upconversion are illustrated in Fig. 3 for Er:YALO. Referring to the ion labeled ‘A’, a pump photon at 507 nm initiates the $^4I_{15/2} \rightarrow ^4I_{9/2}$ transition. The $^4I_{9/2}$ state rapidly relaxes to the intermediate $^4I_{11/2}$ state, which has a lifetime [7] of 1.2 ns. For sequential two-photon absorption upconversion to take place the crystal must be pumped simultaneously at both 507 nm and 540 nm. Pump flux at 540 nm produces the $^4I_{11/2} \rightarrow ^4E_{3/2}$ transition. If the 540 nm flux is sufficiently high, as this is the $^4I_{11/2}$ state will have a greater probability of absorbing a photon than it has of relaxing. The $^4S_{3/2}$ upper laser level is populated by multiphoton relaxation from the $^4E_{3/2}$ state as indicated in Fig. 3.

Cooperative energy transfer upconversion is initiated by absorption at 507 nm. If two neighboring ions (A and B) occupy the $^4I_{11/2}$ state, energy

transfer can occur by a process similar to Auger recombination. As shown by the dashed lines in Fig. 3, cooperative energy transfer upconversion promotes ion B to the $^4F_{7/2}$ state while ion A relaxes to the ground state. Multiphoton relaxation from the



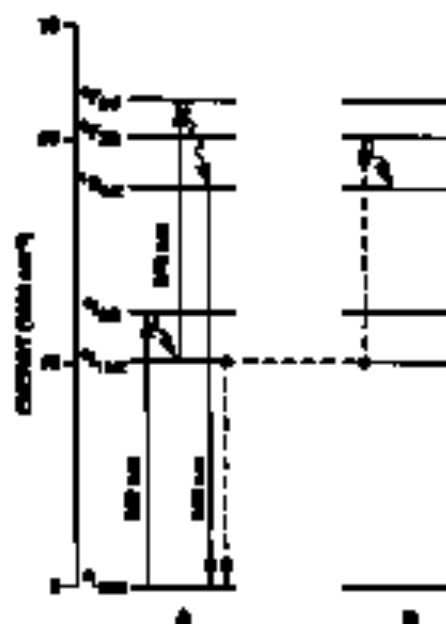


Fig. 3. Upconversion pathway in Br:YALO for sequential one-photon absorption upconversion and cooperative energy transfer upconversion. 'A' and 'B' represent Stark levels. The solid arrows indicate optical transitions, the wavy arrows represent multiphonon relaxation, and the dashed line indicates cooperative energy transfer.

$^4F_{3/2}$ state populates the $^4F_{3/2}$ upper laser level. Energy transfer is easily achieved, generating [1] only 9.3 cm^{-1} of excess energy. The pump efficiency for cooperative upconversion is sensitive to the $^4I_{11/2}$ lifetime, as the excitation of two neighboring ions at the intermediate state and subsequent energy transfer must occur before one of the ions decays.

The wavelengths 300 nm and 340 nm shown in Fig. 3 represent transitions at the lowest Stark level of the respective minimal zone. The range of wavelengths is 285 nm to 307 nm for the five $^4I_{15/2}(1) \rightarrow ^4I_{9/2}(n)$ transitions, and 335 nm to 340 nm for the three $^4I_{11/2}(1) \rightarrow ^4F_{3/2}(n)$ transitions. All wavelengths are designated with their wavenumber values. Laser excitation at 350 nm resonances on the fourth Stark level of the ground state at 212 cm^{-1} . This excitation is the most intense of the eight $^4F_{3/2}(1) \rightarrow ^4I_{15/2}$ fluorescence lines.

Sequential two-photon absorption upconversion pumping had been reported [1] to produce 8 mW of laser output power with an optical conversion effi-

ciency (laser output power as a fraction of incident pump power) of 1.8%. This power was obtained with the crystal at 34 K. Approximately 195 mW of pump power at 789 nm was used to produce the $^4I_{15/2} \rightarrow ^4I_{9/2}$ transition, and 250 mW at 340 nm was used to pump the $^4I_{11/2} \rightarrow ^4F_{3/2}$ transition. The pump flux was generated using a dual wavelength Ti:sapphire laser that produces simultaneous emission at both pump wavelengths. The pump laser is described in more detail in the literature [9,10]. For cooperative energy transfer pumping the upconversion laser output power [2] was 166 mW and the optical conversion efficiency was 1.7%. This performance was achieved using 975 mW of pump power at 307 nm to pump the $^4I_{15/2} \rightarrow ^4I_{9/2}$ transition. The Br:YALO crystal was maintained at 34 K. The dependence of the laser output on pump power is approximately quadratic for cooperative energy transfer, suggesting that optical conversion efficiencies higher than 17% can be produced with higher pump power.

As noted above, photon avalanche upconversion is characterized by absorption at wavelengths mismatch with transitions from a metastable state of the ion. This pump mechanism is illustrated in Fig. 4 for a three-level ion. Assume that ion A occupies metastable level 2. The sample is irradiated with pump flux resonant with the $2 \rightarrow 3$ transition, populating ion A at level 3. Population in level 3 can decay to level 1, producing upconversion emission. Alternatively the ion in level 3 can transfer part of its energy to neighboring ground state ion B by cross relaxation, a process similar to concentration quenching. Cross relaxation energy transfer produces two ions in level 2. Since the level 2 lifetime is long, the two ions can absorb additional pump excitation to produce four in level 2, the four can produce eight, and so on. Under appropriate conditions [11] cross relaxation energy transfer produces an 'avalanche' of population in level 2.

There are two requirements that must be satisfied for photon avalanche upconversion to be effective. The first is that cross relaxation energy transfer must be competitive with the $3 \rightarrow 1$ emission rate. A large cross relaxation rate is inefficient as well as a relatively high Br ion density help satisfy this condition. The second requirement is that the $2 \rightarrow 3$ excitation rate be fast relative to the level 2 lifetime. This condition establishes a pump threshold for photon

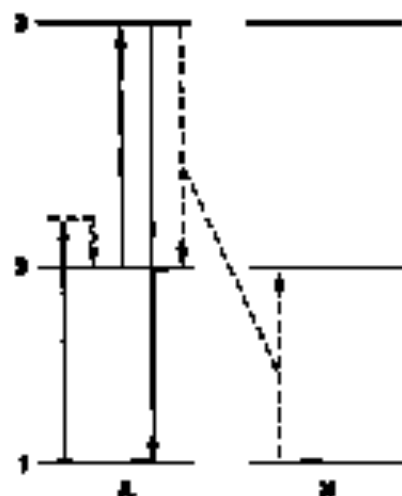


Fig. 4. Schematic representation of phase sensitive operation for a four-level laser. 'A' and 'B' indicate neighboring laser transitions across separate optical resonators and the dotted curves indicate cross relaxation between the two ions. The dotted level 2 shows cooperative level 2 representing the excited energy of the up-conversion absorption transition.

avalanche upconversion. A long detectable both filaments and a large absorption cross section serve to reduce the magnitude of the threshold pump intensity.

It was assumed that ion A starts out in level 2, and indeed a small population in this level is required to initiate phase sensitive upconversion. This population is produced by non-resonant absorption of pump flux by ions in the ground state as illustrated in Fig. 4.

Both sequential two-photon absorption upconversion and cooperative energy transfer upconversion involve optical pumping from the $^4I_{13/2}$ ground state. The criterion that a distinct, third pump transition produces upconversion laser emission in Er:YALO includes the assignment of the resonant pump transitions as neighboring in the $^4I_{13/2}$ manifold state as well as the substantial differences in the parametric dependence of upconversion laser emission initiated by resonant cross absorption (MSA) compared to that produced by ground state absorption. For example, the temperature dependence of the laser output power goes through a peak at 34 K when the pump mechanism is cooperative energy transfer upconversion [1]. On the other hand, for upconversion emission involving MSA the laser

output power decreases monotonically [2] with temperature. The highest laser output power was obtained at 5.7 K, the lowest temperature produced by the crystal. The output power was 33 mW and was produced with a pump wavelength of 791.3 nm.

MSA-initiated upconversion in Er:YALO is illustrated in Fig. 5. Five wavelengths resonant with transitions from the $^4I_{13/2}$ state produce upconversion laser emission. These wavelengths are 796.2 nm, 794.4 nm, 791.3 nm, 789.1 nm and the odd 787.4 nm, and correspond to transitions from the first Stark level of the $^4I_{13/2}$ state to the second through the sixth Stark levels of the $^2H_{11/2}$ state, respectively. Emission resonant with transitions to the first Stark level of the $^2H_{11/2}$ state produces 150 nm fluorescence but not upconversion laser emission [2]. The 150 nm intense emission is generated by pumping at 791.3 nm, and this wavelength was used for most of the fluorescence measurements.



Fig. 5. Upconversion in Er:YALO initiated by resonant cross absorption. Solid curves represent optical transitions, wavy curves indicate equilibrium relaxation and the dotted line represents cross relaxation energy transfer. The $^4I_{13/2}$ state is resonant.

Referring to Fig. 5, non-resonant absorption of the pump flux by ground state ions followed by relaxation from the ${}^4I_{9/2}$ state populates the ${}^4I_{11/2}$ metastable state. Resonant absorption of a 791.3 nm photon promotes ion A from the ${}^4I_{13/2}(1)$ level to the ${}^2I_{11/2}(4)$ state. The ${}^4I_{13/2}$ state has a lifetime [12] of 7.2 ns. Relaxation from the ${}^2H_{11/2}$ state to the ${}^4S_{3/2}$ state and subsequent radiative decay to the ${}^4I_{15/2}$ state produce upconversion emission. Alternatively, population in the ${}^4S_{3/2}$ state can participate in cross relaxation energy transfer with neighboring ground state ion B to produce ion loss in the ${}^4I_{13/2}$ state. As illustrated in Fig. 5, ion B is promoted to the ${}^4I_{15/2}$ state directly while ion A populates the ${}^4I_{13/2}$ state by activation from the ${}^4I_{11/2}$ state. The excess energy produced by cross relaxation from the ${}^4S_{3/2}$ state is approximately 1500 nm^{-1} .

Although not illustrated, cross relaxation from the ${}^2H_{11/2}$ state can occur as well. In this case cross relaxation energy transfer initially produces population in the ${}^4I_{15/2}$ state (ion A) and the ${}^4I_{11/2}$ state (ion B). Spontaneous relaxation from the ${}^4I_{9/2}$ state populates the ${}^4I_{13/2}$ state. Cross relaxation from the ${}^2H_{11/2}$ state is nearly resonant, generating only 4.3 nm^{-1} of excess energy.

As noted above, MSA-initiated upconversion in Er:YALO had been previously assigned [2] to photon avalanche pumping. Indeed the kinetic processes illustrated in Fig. 3 show several scenarios to coexist with photon avalanche. However, it is important to note that population in the ${}^4I_{13/2}$ state may be produced by both cross relaxation energy transfer from the ${}^4S_{3/2}$ state and non-resonant absorption from the ground state even though photon avalanche does not take place. Reproducing the metastable state population is essential for laser operation, as the upper laser level is fed by resonant absorption of pump flux by ${}^4I_{13/2}$ ions. The population inversion in the ${}^4S_{3/2}$ state is maintained in the absence of photon avalanche pumping due in part to the relatively large cross section for the ${}^4I_{13/2} \rightarrow {}^4I_{9/2}$ non-resonant absorption.

Experimental results will be presented below which contrast the association of photon avalanche pumping with MSA-initiated upconversion in Er:YALO. This is followed by a description of the energy flow pathways that produce upconversion emission.

4. Results

Two types of fluorescence measurements can be used to establish photon avalanche upconversion pumping. The first is the observation of a threshold in the dependence of the upconversion fluorescence on pump power. The data produced by such a measurement are illustrated schematically in Fig. 6. At low pump power the fluorescence intensity varies quadratically, but as the pump power continues to increase a transition point is reached. The onset of the transition region marks the photon avalanche threshold pump power as described in the previous section. As the pump intensity increases well beyond threshold the upconversion emission intensity is once again characterized by a quadratic dependence on pump power.

The absence of a threshold in the pump power dependence is not sufficient to rule out photon avalanche as the dominant upconversion pump mechanism. The temporal dependence of the fluorescence intensity provides a definite indication of photon avalanche upconversion pumping. Two examples are illustrated schematically in Fig. 7. In Fig. 7A the increase in the fluorescence with time is shown for the case where photon avalanche upconversion is not taking place, while Fig. 7B illustrates the fluorescence rise expected when photon avalanche pumping occurs. In the latter case the concave region of the fluorescence dependence is produced by the initial exponential growth of population in the metastable state. The temporal dependence of the upconversion fluorescence will resemble Fig. 7B for pump powers that exceed the photon avalanche threshold.

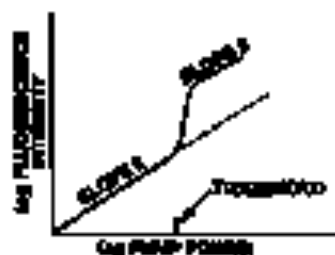


Fig. 6. Schematic illustration of the dependence of the fluorescence intensity on pump power when photon avalanche upconversion pump power occurs. Both axes are logarithmic.

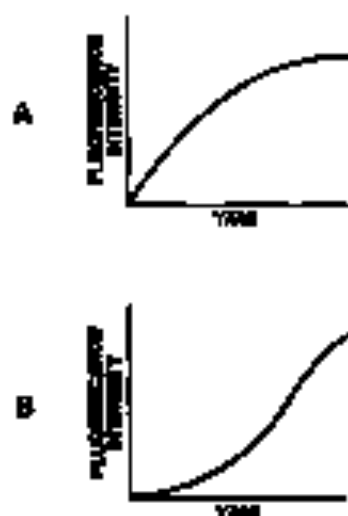


Fig. 7. Schematic illustration of the complex dependence of the upconversion fluorescence intensity for the case where photonic avalanche does not occur (A) and the case where the photonic avalanche threshold is exceeded (B).

Fig. 8 shows the increased pump power dependence of the Er:YALO upconversion fluorescence. The pump wavelength is 791.3 nm and the crystal temperature is 7 K. A line of slope 2 is drawn to illustrate the approximately quadratic dependence of the fluorescence intensity on pump power. The data do not indicate the presence of a pump threshold. Data taken using other 532 nm pump wavelengths produced plots similar to that shown in Fig. 8.

The temporal dependence of the fluorescence is illustrated in Fig. 9 for upconversion produced by two different pump wavelengths. For Fig. 9A the pump wavelength is 307 nm and cooperative energy transfer is the dominant pump mechanism. For Fig. 9B the pump wavelength is 791.3 nm. Figs. 9A and 9B each contain two traces: the upper trace represents the fluorescence pulse while the lower trace represents the pump pulse. The fluorescence detector pulse polarity is negative and has a baseline approximately coincident with the first horizontal grid line below the top of the oscillogram traces. In Fig. 9A the fluorescence intensity increases rapidly after the sharper pump and reaches steady state as $1 - e^{-t/\tau}$, where τ is the lifetime of the $^4I_{11/2}$ state. The slow decay of the 550 nm fluorescence following pump pulse termination is characteristic of cooperative energy transfer upconversion and is due to ions in the

long-lived $^4I_{11/2}$ state continuing to feed the $^4F_{3/2}$ state.

In Fig. 9B the time required to reach steady state is longer due to the 7.3 ns lifetime of the $^4I_{13/2}$ state. The rapid decay of the emission following termination of the 791.3 nm excitation pulse indicates that cooperative energy transfer does not produce significant upconversion emission at this pump wavelength. The onset of 550 nm fluorescence does not display a concave region of the type illustrated in Fig. 7B. Data similar to that shown in Fig. 9B were obtained for pump wavelengths corresponding to transitions to the other Stark levels of the $^2E_{11/2}$ state. For all excitation wavelengths the slope of the temporal fluorescence curve was not sensitive to pump power up to the maximum pump power available (approximately 900 mW). Clearly photonic avalanche upconversion does not take place.

The temporal dependence of the fluorescence at 550 nm due to the $^4F_{3/2} \rightarrow ^4I_{15/2}$ emission, and at 973 nm due to the $^4I_{11/2} \rightarrow ^4I_{13/2}$ transition, were also measured. The traces are similar to that shown

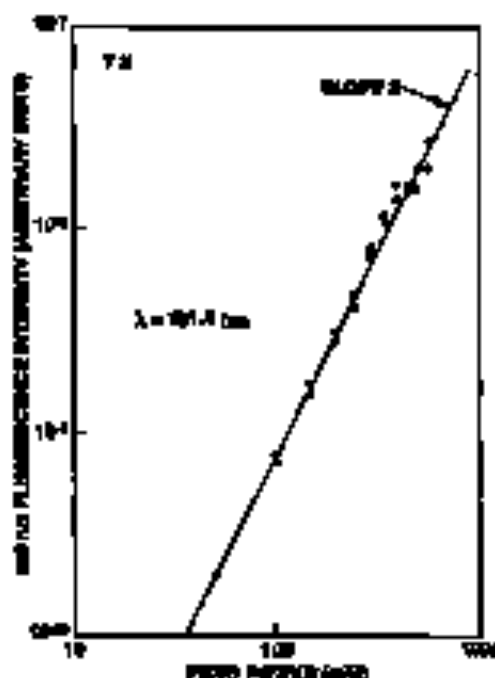


Fig. 8. Variation of the 550 nm emission intensity with pump power for Er:YALO. Solid line is drawn to illustrate a slope of 2. Both axes are logarithmic, and the pump wavelength is indicated.

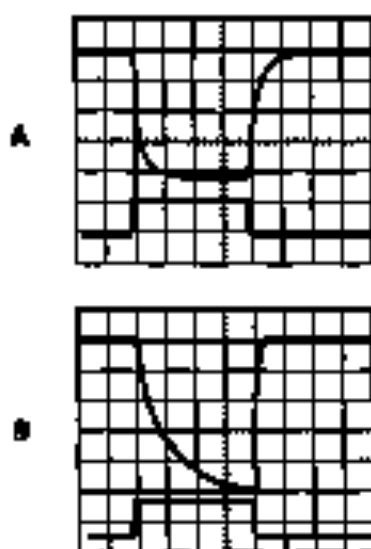


Fig. 9. Temporal structures of the 337 nm excimer laser pulses. The upper trace in each oscillogram represents the fluorescence pulse detected with a PMT and the lower trace represents the pump pulse detected with a photodiode. The PMT produces a negative signal when fluorescence is detected while the photodiode produces a positive signal when the pump is on. The rise time is 2 ns/step for both oscillograms. The acquisition rate is 337 ns/div for oscillogram A and 297.3 ns/div for oscillogram B.

In Fig. 9A or Fig. 9B depending on whether the pump transition originates in the ${}^4I_{13/2}$ or ${}^4I_{9/2}$ state respectively. We also measured the temporal dependence of the fluorescence at 1.3 μm due to the ${}^4I_{13/2} \rightarrow {}^4I_{9/2}$ transition. Emission was detected using a Ge photodiode in conjunction with an interference filter centered at 1.372 μm . The FWHM of the filter was 83 nm. For pump wavelengths resonant with ground state absorption the temporal dependence of the 1.3 μm emission was similar to that shown in Fig. 9A. However, no emission at 1.3 μm could be measured when the pump wavelength was resonant with transitions from the ${}^4I_{11/2}$ state.

Non-resonant absorption by ground state Er^{3+} ions plays an important role in the MSA-induced upconversion pump mechanism. To gauge the relative magnitude of the non-resonant pump and the pump wavelength was detuned from one of the MSA lines by an amount sufficient to inhibit upconversion fluorescence. Emission in the 970 nm band due to the ${}^4I_{11/2} \rightarrow {}^4I_{13/2}$ transition was used

to provide a measure of the strength of the non-resonant ${}^4I_{13/2} \rightarrow {}^4I_{9/2}$ transition illustrated in Fig. 3. Following absorption the ${}^4I_{9/2}$ level relaxes rapidly and efficiently to the ${}^4I_{11/2}$ level. Emission at 970 nm is therefore due entirely to non-resonant absorption under conditions where no upconversion pumping occurs.

An S-1 PMT was oriented at 90° with respect to the emission axis and was used in conjunction with a filter to block wavelengths shorter than 970 nm. The pump wavelength was set to 297.3 nm, i.e. 40 nm higher than the 256.3 nm MSA line and approximately 3 nm detuned from the nearest ground state transition. Emission at 970 nm is shown in Fig. 10A. The slow rise and fall times indicate that the signal is dominated by fluorescence rather than scattered pump light. Fig. 10B shows the PMT output obtained with a pump wavelength of 330 nm. This pump wavelength is almost a factor of three further detuned from the nearest ground state transition than the 297.3 nm excitation wavelength. At 330 nm there

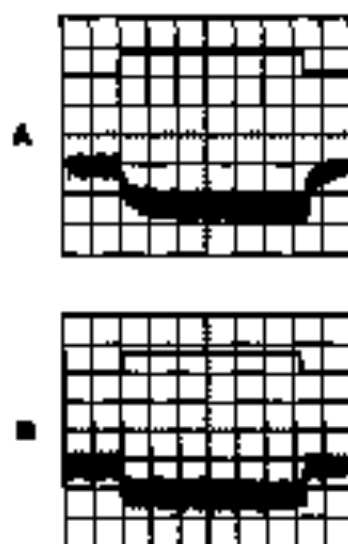


Fig. 10. Fluorescence produced by non-resonant excitation. Both oscillograms were taken on the same. The upper trace represents the pump intensity excitation, while the lower trace represents the PDM and fluorescence. The detector polarity in both cases is negative. The 297.3 nm trace for each oscillogram is 2 ns/step. The oscillogram gain is increased for the fluorescence signal in (B) relative to (A). (A) Fluorescence at 970 nm using a pump wavelength of 297.3 nm. (B) PMT signal for a pump wavelength of 330 nm.

be higher than would otherwise be expected. Although the upper state lifetime is short, the pump flux populates the ${}^2F_{11/2}$ state directly. A high pump photon density might provide a sufficient steady state population in this level. Indeed, the flux that at 1.5 μm radiation is observed when the pump wavelength is resonant with one of the MSA transitions is consistent with a high MSA pump rate.

We attempted to use fluorescence from the ${}^2F_{11/2}$ state to determine whether a measurable population in this level is maintained when the pump wavelength is resonant with one of the MSA transitions. Emission from the ${}^2F_{11/2}$ state is generally weak, and the fluorescence spectrum was first taken at room temperature to identify an emission line that could be used to monitor the ${}^2F_{11/2}$ population. The 700 cm^{-1} energy gap between the ${}^4S_{3/2}$ state and ${}^2F_{11/2}$ state allows a relatively high thermal population in the latter state at room temperature under excitation conditions that produce a steady state population in the ${}^4S_{3/2}$ state. A weak fluorescence peak at 728.1 nm was observed when the room temperature Er:YALO crystal was excited at 807 nm. This wavelength corresponds to the ${}^2F_{11/2}(1) \rightarrow {}^4I_{15/2}(4)$ transition. The crystal was cooled to 7 K and excited with pump radiation in the 800 nm band. Pump wavelengths resonant with either ground state or metastable state absorption were used, but no 728.1 nm emission was observed at this temperature.

In the course of searching for low level fluorescence from the ${}^2F_{11/2}$ state we detected upconversion fluorescence due to the ${}^2P_{3/2} \rightarrow {}^4I_{15/2}$ transition. The ${}^2P_{3/2}(1)$ level is at 31 449 cm^{-1} and five emission lines are produced near 530 nm. Emission from the ${}^2P_{3/2}$ state was obtained with a pump wavelength of 807 nm but not for the MSA pump wavelength at 790.2 nm. The intensity of the 530 nm fluorescence is more than two orders of magnitude below the 530 nm emission from the ${}^4S_{3/2}$ state. The fluorescence spectra are shown in Fig. 12.

5. Discussion

5.1. Mechanism for MSA-initiated upconversion

The fluorescence data confirm that a mechanism other than photon avalanche pumping produces up-

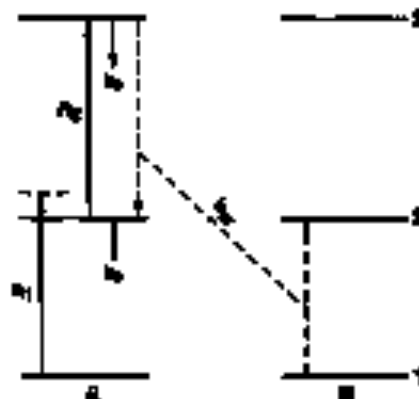


Fig. 13. Processes involved in MSA-initiated upconversion for a three-level ion. R_1 and R_2 represent absorption, R_3 and R_4 represent single ion decay processes from levels 3 and 2, respectively, and the dashed line indicates cross relaxation.

conversion emission in Er:YALO. Non-resonant sequential two-photon absorption upconversion is consistent with MSA-initiated pumping and is illustrated in Fig. 13 for a three level ion. The crystal is pumped at a wavelength resonant with the 2 \rightarrow 3 transition. Non-resonant absorption by ground state ions populates level 2 with a pump rate coefficient of R_1 , and ions in level 2 are promoted to upper laser level 3 with rate coefficient R_2 . Fluorescent non-resonant two-photon absorption is common [6] in transparent fiber lasers. For three lasers room temperature operation provides a substantial non-resonant absorption rate due to the numerous broad absorption lines. Although the non-resonant transition rate is relatively large in Er:YALO, this rate is only a small fraction of the resonant absorption rate. It is therefore unlikely that laser emission could be sustained by non-resonant sequential two-photon absorption operating alone.

However, in Er:YALO the metastable state population produced by non-resonant sequential two-photon absorption is enhanced by contributions due to cross relaxation energy transfer. Cross relaxation is a pair mechanism, producing two ions in the metastable state for each energy transfer interaction involving an excited (level 3) ion. It is likely that both of these pump mechanisms operate simultaneously to produce the ${}^4S_{3/2}$ state population sufficient to sustain laser emission.

Er:YALO is unusual in that the non-resonant absorption rate coefficient R_1 is not negligible rela-

sive to the resonant absorption rate coefficient R_2 . This is not seen at cryogenic temperatures and results from the proximity of the ${}^4I_{11/2} \rightarrow {}^4I_{9/2}$ and ${}^4I_{13/2} \rightarrow {}^2H_{11/2}$ transition wavelengths. Recently, Breiner and Janyk [15] modeled upconversion in Er:YALO. Their model is consistent with the experimental observations reported in this work, and indicates that a large non-resonant absorption rate coefficient has the effect of increasing the pump threshold for photon avalanches. When the ratio of R_2/R_1 is less than 10, photon avalanche upconversion may not occur at any pump power level.

For room temperature upconversion in Er:YALO pumped with 635 mW of laser power at 796.2 nm, Breiner and Janyk used $R_2/R_1 = 2$ and calculated the fractions of ${}^4S_{3/2}$ population produced by cross relaxation and non-resonant sequential two-photon absorption to be 0.77 and 0.23, respectively. The relative magnitude of the non-resonant absorption rate is consistent with published room sections for Er:YALO [16] and Er:YLF [17].

The proposed upconversion pump mechanism involves recycling or 'looping' of excitation between the upper laser level (or, alternatively, the ${}^2H_{11/2}$ state) and the metastable state. Cross relaxation from the upper level produces ions in the ${}^4I_{13/2}$ state, while subsequent absorption of pump photons repopulates the upper level. Loop gain results from the production of two metastable ions by cross relaxation between an ion in the upper level and one in the ground state, and ions in produced by upconversion excitation from the upper laser level to the ground state. Additional population in the metastable state is produced by non-resonant ground state absorption.

Looping through the emission channel and least discussed in relation to the 2.8 μm ${}^4I_{11/2} \rightarrow {}^4I_{13/2}$ Er laser transition [18]. The 2.8 μm laser is produced by optical pumping at 800 nm to populate the ${}^4I_{9/2}$ state. As noted above, this state relaxes to the ${}^4I_{11/2}$ upper laser level. As an alternative to relaxation, as ions in the ${}^4I_{9/2}$ state can produce two ions in the ${}^4I_{13/2}$ terminal laser level by cross relaxation with a ground state ion. Cooperative upconversion between two ions in the ${}^4I_{13/2}$ state repopulates the ${}^4I_{9/2}$ state. The looping mechanism in the 2.8 μm laser compares cross relaxation to the lower level followed by cooperative upconversion to the upper

level. This looping model is consistent with the observation of higher laser efficiency using a longer pump wavelength to excite the ${}^4I_{11/2}$ state directly (~ 970 nm), since in that case the terminal laser level is not populated by cross relaxation from the ${}^4I_{9/2}$ state. It is consistent as well with the observation of cw lasing at 2.8 μm despite the longer lifetime of the terminal laser level relative to the ${}^4I_{11/2}$ upper laser level. Classically such systems cannot [19] operate cw, but cooperative upconversion serves [20] to shorten the effective lifetime of the ${}^4I_{13/2}$ state.

Looping has also been discussed [21] in detail for systems that undergo only noncooperative energy transfer-upconversion. In this model decay from the upper level to the metastable level occurs by a cascade involving both multiphonon relaxation and radiative emission. Cooperative upconversion involving ions in the metastable level re-populates the upper level, completing the energy loop. Looping is shown by the authors [21] to result in enhanced quantum efficiency as well as causing certain transient effects in the laser output.

No evidence was found to support significant participation of the ${}^2H_{11/2}$ state in the cross relaxation energy transfer pathway. The experimental results are somewhat inconclusive. However, to the fluorescence that was used to monitor the ${}^2H_{11/2}$ population is weak. The energy resonance of the initial and final states involved in cross relaxation from the ${}^2H_{11/2}$ state, coupled with the observation that the ${}^2H_{11/2}$ state is the resonant level for the optical pump transition, support the participation of that quenching pathway. It is of interest to note that both excited state absorption [17] and cross relaxation [18] involving the short-lived [20] ${}^4I_{9/2}$ state was reported to contribute to the upconversion pump dynamics in Be-doped crystals.

A previous attempt [2] to determine whether the ${}^2H_{11/2}$ state participates in cross relaxation was also inconclusive. In that experiment excitation at 847 nm was used in an effort to pump the ${}^4I_{13/2}(1) \rightarrow {}^4S_{3/2}(1)$ transition. If upconversion excitation had been observed the energy transfer pathway involving the ${}^2H_{11/2}$ state could be illustrated. However, no upconversion could be detected in light of the description of the MSA-initiated pump mechanism described above, it can be recognized that the failure of

pump light at 847 nm, its probable upconversion may be a reflection of the substantially lower non-resonant absorption rate from the ground state. It does not necessarily suggest that the $^4S_{3/2}$ state is not involved in cross relaxation. The non-resonant absorption cross section varies [17] as $\exp(-\alpha \Delta E)$, where α is a constant and ΔE represents the energy difference between the pump photon and the nearest ground state transition. For a pump wavelength of 847 nm the energy difference is approximately 600 cm^{-1} compared to one of 200 cm^{-1} for the MFA laser near 800 nm.

5.2. The role of energy recycling in cooperative upconversion pumping

Cross relaxation from the $^4S_{3/2}$ state is an effective energy transfer mechanism. Concentration quenching was reported [22] to reduce the fluorescence lifetime of the $^4S_{3/2}$ state in a 1.5% doped Er:YALO crystal to 30 μs from the low concentration lifetime of 160 μs . Ansel and Chen [7] estimate that the unmodified ($n_1 = 1$) cross relaxation rate coefficient for Er:YLF is $5 \times 10^6 \text{ s}^{-1}$.

Although efficient cross relaxation is important for MFA-initiated upconversion, it is a loss mechanism for cooperative energy transfer upconversion. When the Er:YALO crystal is pumped [1] by wavelength resonant with transitions from the ground state, cooperative energy transfer pumping dominates the concentration dynamics. Recall that cooperative energy transfer upconversion requires one ion in the $^4I_{11/2}$ state to produce an ion in the $^4S_{3/2}$ state. Cross relaxation removes population from the $^4S_{3/2}$ state and therefore increases the effective number of pump photons required to produce a visible photon.

Despite upper laser level population loss by cross relaxation, cooperative energy transfer pumping in Er:YALO has produced the highest optical conversion efficiency reported for an upconversion laser [1,2]. The reason for this apparent contradiction is that the quenching produces little much of the $^4S_{3/2}$ state level energy within the pump-dynamics loop, allowing the upper laser level to be re-populated. Excitation is recycled by cooperative upconversion involving the quenching products.

Quenching initially produces one ion in the $^4I_{11/2}$ state and one in the $^4I_{13/2}$ state. The ion in the $^4I_{11/2}$

state can participate in cooperative energy transfer with a neighboring ion in the $^4I_{11/2}$ state to re-populate the $^4S_{3/2}$ state. Alternatively, the ion can decay to the $^4I_{13/2}$ state. If the $^4I_{11/2}$ ion relaxes, the $^4I_{11/2}$ state can be re-populated by cooperative energy transfer with another ion in the $^4I_{13/2}$ state. Cooperative energy transfer upconversion between neighboring ions in the $^4I_{13/2}$ state is efficient in Er-doped crystals, and it was reported [20] that this energy transfer process determines the population inversion kinetics of the Er³⁺ $^4I_{11/2} \rightarrow ^4I_{13/2}$ 2.8 μs laser transition. Alternatively, ions lost in the $^4I_{13/2}$ state can participate in a 'trio' upconversion process to produce an ion in the $^4S_{3/2}$ state directly. Efficient 350 nm laser emission has been demonstrated [23] in Er:YLF using trio upconversion pumping at 1.55 μm .

If the cross relaxation-produced ion in the $^4I_{11/2}$ state undergoes a second cooperative energy transfer interaction to re-populate the $^4S_{3/2}$ state, the reduction in pump quantum efficiency may be as little as 11%. To see this, note that in the absence of cross relaxation two 600 nm photons are required to produce an ion in the $^4S_{3/2}$ state. When cross relaxation occurs, a third pump photon is needed to re-populate the $^4S_{3/2}$ state. The third photon produces a ground state ion in the $^4I_{11/2}$ state, in this case three pump photons produce an ion in the $^4S_{3/2}$ state plus one ion in the $^4I_{11/2}$ state. Based on the trio process, the ion in the $^4I_{13/2}$ represents one-third of the photons required to produce another ion in the $^4S_{3/2}$ state. For this process then, three pump photons produce $1/3$ ion in the $^4S_{3/2}$ state and the quantum loss is 11% relative to the quenching-free excitation pathway. Similarly we can calculate the quantum loss for other pathways for repopulating the $^4S_{3/2}$ state. These losses range up to 33% as long as either cross relaxation-produced ion returns back to the $^4I_{13/2}$ ground state. Recycling dynamics have been discussed in previous papers [18,20,21] on Er-doped lasers.

Having described the effect of cross relaxation on reducing the efficiency of cooperative energy transfer upconversion pumping, we note that cooperative energy transfer involving ions in the $^4I_{11/2}$ state requires a loss mechanism for the MFA-initiated pump process described in Section 5.1. Population in the $^4I_{13/2}$ metastable state is required to recycle

upconversion, as the pump wavelength is resonant with transitions from this state. To the extent that cooperative energy transfer depletes the metastable state population, the pump efficiency will be reduced. This reduction is analogous to that described above in the additional pump photons are required to produce a visible photon, although in this case it is due to laser crystal absorption.

Only a small reduction in the efficiency of MSA-initiated upconversion is expected to result from cooperative energy transfer. This is due to the lower steady state density of $^4I_{13/2}$ ions relative to the case where cooperative energy transfer dominates the upconversion pump dynamics. The lower metastable state density was demonstrated by the 1.5 μm up-conversion experiment reported above. The optical flux used for MSA-initiated pumping is resonant with the $^4I_{13/2} \rightarrow ^2H_{11/2}$ transition and effectively depletes the steady state metastable population.

5.3 Cooperative energy transfer pathway of the $^2P_{3/2}$ state

The appearance of the $^2P_{3/2} \rightarrow ^4I_{13/2}$ emission lines produced by excitation at 807 nm and not at 796.2 nm is an observation that provides some insight into the upconversion population dynamics of the $^2P_{3/2}$ state. Since both pump wavelengths populate the $^4S_{3/2}$ state it is not likely that cooperative energy transfer between neighboring $^4S_{3/2}$ ions produces the $^2P_{3/2}$ state. The most significant difference in the ionic state populations between the energy transfer pathways associated with the two pump wavelengths is the population in the $^4I_{13/2}$ state. As noted, this metastable state ion density is depleted under MSA-initiated pumping compared to cooperative energy transfer pumping.

The cooperative upconversion between an ion in the $^4S_{3/2}$ state and two in the $^4I_{13/2}$ state is the most likely pathway for populating the $^2P_{3/2}$ state, as most other upconversion pathways can be readily eliminated. For example, cooperative upconversion involving ions in states that lie above the $^4S_{3/2}$ state is unlikely due to the short lifetimes of these levels. For the longer lived ground state, the lifetime of the $^2P_{3/2}$ state [7] is 1.2 μs in Er:YALO. While the lifetimes of the $^4G_{11/2}$ and $^4F_{3/2}$ states in Er:YLF [24] are 7 μs and 9 μs , respectively. Cooperative

energy transfer among ions in the $^4I_{13/2}$ state would require that five neighboring metastable state ions participate to produce an ion in the $^2P_{3/2}$ state. Cooperative upconversion from the $^4I_{11/2}$ state is also unlikely as four neighboring ions in that state would have to participate. Alternatively, the upconversion can occur among a $^4S_{3/2}$ state ion and two in the $^4I_{11/2}$ state. However, this pathway is less likely than the upconversion involving $^4I_{13/2}$ state ions. The $^4I_{11/2}$ state lifetime is shorter, and 7900 cm^{-1} of additional excess energy is produced by this process. In addition, if this pathway were effective it might be expected to produce $^2P_{3/2}$ emission when pumping at 796.2 nm as well as at 807 nm. This upconversion from the $^4P_{3/2}$ state could also produce the $^2P_{3/2}$ state. This is unlikely due to the 19 μs lifetime [7] of this state as well as the large excess energy that would be produced. The nearest electronic level that could be populated is the $^4D_{3/2}$ state, which lies [25] almost 9000 cm^{-1} lower in energy.

Upconversion from the $^2P_{3/2}$ state has also been observed in Er:YLF. Emission at 670 nm is due to the $^2P_{3/2} \rightarrow ^4I_{11/2}$ transition. It was proposed [26] that population of the $^2P_{3/2}$ state occurs via a multi-step upconversion pump mechanism. In the first step, two neighboring ions in the $^4I_{11/2}$ state produce the $^4S_{3/2}$ state by cooperative energy transfer upconversion. The second step comprises cooperative upconversion between an ion in the $^4S_{3/2}$ state and one in the $^4F_{9/2}$ state. This mechanism is less likely to occur in Er:YALO than the three-step upconversion mechanism suggested above for two reasons. First, the two states involved in the proposed upconversion mechanism, the $^4I_{11/2}$ and $^4F_{9/2}$, have significantly shorter lifetimes than the $^4I_{13/2}$ and $^4S_{3/2}$ states, respectively. The lifetimes of the four states are: 1.2 ns, 19 μs , 7.2 ns and 160 μs , respectively. Second, if the proposed mechanism described the population kinetics of the $^2P_{3/2}$ state upconversion emission would be produced when pumping at 796.2 nm as well as at 807 nm. This is not observed.

6. Summary and conclusions

Upconversion fluorescence initiated by absorption from the $^4I_{13/2}$ metastable state has been character-

used in Er:YALO. Pump wavelengths used were 796.2 nm, 794.4 nm, 791.3 nm, 789.1 nm and 787.4 nm. The data suggest that the upconversion pump mechanism involves both cross relaxation energy transfer and non-resonant sequential two-photon absorption. This mechanism is somewhat similar to photon avalanche upconversion pumping, but is characterized by relatively high non-resonant ground state absorption. As a result there is no upconverted pump intensity threshold. This pump mechanism has not been previously identified with producing upconversion laser emission in a crystalline laser.

Cross relaxation energy transfer was discussed in terms of its impact on the efficiency of cooperative energy transfer upconversion pumping. The role of energy recycling in mitigating the pump efficiency losses was described. The pathways for upconversion pumping of the $^2F_{3/2}$ state in Er:YALO were also discussed. The most likely pump mechanism is intracenter energy transfer involving rare ions in the $^4I_{13/2}$ state and on ions in the $^4S_{3/2}$ state.

Acknowledgements

This work was supported in part by the Office of Naval Research. The author wishes to thank Dr. Mihai Koles of Union Carbide for providing the Er:YALO crystal.

References

- [1] B. Schapp, IEEE J. Quantum Electron. 20 (1984) 2914.
- [2] B. Schapp, IEEE J. Quantum Electron. 31 (1985) 208.
- [3] H. Becht, G. Haugam, J. Kneip, G. Hense and H. Lenz, Appl. Phys. Lett. 10 (1980) 2280.
- [4] H.P. Hoop, P. Zhou, H.S.P. Cheng and H. Lenz, Opt. Lett. 18 (1993) 112.
- [5] A.J. Ghossein, W. Lohjck and H.M. Hechtner, Appl. Phys. Lett. 51 (1987) 1027.
- [6] H. Stumpf, Progr. Quantum Electron. 20 (1986) 271.
- [7] M.J. Weber, Phys. Rev. B 8 (1973) 54.
- [8] V.L. Ivanov and A.G. Savelov, J. Chem. Phys. 37 (1973) 4777.
- [9] B. Schapp and J.P. Meyer, IEEE Photonics Tech. Lett. 4 (1992) 1.
- [10] B. Schapp and J.P. Meyer, IEEE J. Quantum Electron. 20 (1984) 1810.
- [11] M.F. Jacob, S. Day and B. Joplin, Phys. Rev. B 42 (1990) 10291.
- [12] K.A. Payne, L.L. Chase, L.K. Becht, W.L. Homy and W.P. Krivan, IEEE J. Quantum Electron. 11 (1983) 2169.
- [13] W. Lohjck and H.M. Hechtner, J. Lumin. 45 (1989) 345.
- [14] U. Gellner, M.J. Riley, F.S. Moy and M.J. O'Keefe, J. Lumin. 15 (1982) 261.
- [15] A. Brueck and A.M. Jacqz, Phys. Rev. B, to be published.
- [16] M. Parnian, E. Reichman and G. Haber, Appl. Phys. A 54 (1992) 405.
- [17] P. Avand and Y. Chou, J. Lumin. 48 (1992) 45.
- [18] K.C. Bowman and J. Burroughs, Opt. Lett. 17 (1992) 818.
- [19] J.T. Vanhyon, Laser Electronics (Prentice-Hall, Englewood Cliffs, 1983) pp. 165-171.
- [20] K.A. Parfitt and D.B. Chang, Opt. Quantum Electron. 22 (1980) 578.
- [21] P. Min and S.C. Reid, J. Opt. Soc. Am. B. 11 (1994) 901.
- [22] M.J. Weber, M. Weber, T.H. Woodman and G.P. Blau, IEEE J. Quantum Electron. 9 (1973) 1038.
- [23] P. Min and S.C. Reid, Opt. Lett. 17 (1992) 1198, 1223.
- [24] C. Li, Y. Geyin, C. Lindeke, H. Mueccorg and M.J. Weber, Opt. Soc. Am. Proc. Adv. Solid State Lasers. 13 (1992) 91.
- [25] G.H. Brown and H.M. Crossman, Appl. Opt. 3 (1963) 875.
- [26] T. Harbur, R. Wawonzone, W. Lohjck and H.M. Hechtner, Appl. Phys. Lett. 57 (1990) 1727.